Infrared Spectroscopic Evidence of a Redox-Dependent Conformational Change Involving Ion Binding Residue NqrB-D397 in the Na+-Pumping NADH:Quinone Oxidoreductase from Vibrio choler...

Infrared Spectroscopic Evidence of a Redox-Dependent Conformational Change Involving Ion Binding Residue NqrB-D397 in the Na⁺-Pumping NADH:Quinone Oxidoreductase from *Vibrio cholerae*

Yashvin Neehaul,[†] Oscar Juárez,[‡] Blanca Barquera,[‡] and Petra Hellwig*,[†]

[†]Laboratoire de bioelectrochimie et spectroscopie, UMR 7140, Chimie de la Matière Complexe, Université de Strasbourg-CNRS, Strasbourg, France

[‡]Department of Biology, Center for Biotechnology and Interdisciplinary Studies, Rensselaer Polytechnic Institute, Troy, New York 12180, United States

S *Supporting Information*

ABSTRACT: The Na⁺-pumping NADH:quinone oxidoreductase (Na⁺-NQR) is a unique respiratory enzyme that conserves energy by translocating Na⁺ through the plasma membrane. Found only in prokaryotes, the enzyme serves as the point of entry of electrons into the respiratory chain in many pathogens, including *Vibrio cholerae* and *Yersinia pestis*. In this study, a combined electrochemical and Fourier transform infrared (FTIR) spectroscopic approach revealed that Na⁺-NQR undergoes significant conformational changes upon oxidoreduction, depending on the monovalent cation present (Na⁺, Li⁺, K⁺, or Rb⁺). In the presence of the inhibitor Rb⁺, additional conformational changes are evident, indicating a changed accessibility of the sodium binding sites. In electrochemically induced FTIR difference spectra, the involvement of deprotonated acid residues in the binding of cations, together with the spectral features, that point toward a monodentate binding mode for these acid residues in the oxidized form of the enzyme and bidentate binding in the reduced form could be identified. The measurements confirmed that NqrB-D397 is one of the acid residues involved in Na⁺ and Li⁺ binding. In the NqrB-D397E mutant, the spectral features characteristic of COO⁻ groups are shifted, and a weakening of the hydrogen binding of the ion binding cluster is revealed. Finally, H−D exchange kinetics of amide protons confirmed that Na⁺-NQR adopts different conformations, with different accessibilities to the aqueous environment, depending on the cation present, which contributes to the selectivity mechanism of ion translocation.
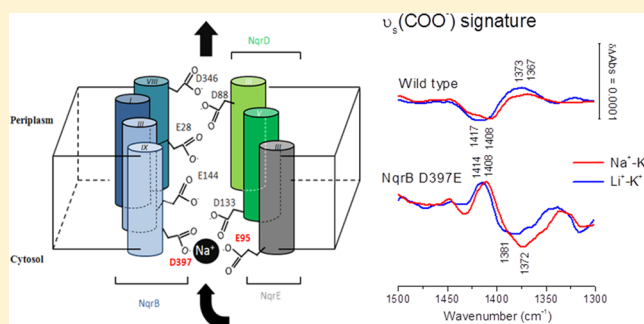
The Na⁺-pumping NADH:quinone oxidoreductase (Na⁺-NQR) is the point of entry of electrons into the respiratory chains of many marine and pathogenic organisms, including *Yersinia pestis*, *Haemophilus influenzae*, and *Vibrio cholerae*.[1,2] Na⁺-NQR is analogous to complex I, in that it accepts electrons from NADH and transfers them to the ubiquinone pool. However, instead of pumping H⁺ across the membrane, Na⁺-NQR translocates Na⁺. The resulting electrochemical sodium gradient provides energy for vital processes, including ATP synthesis, uptake of nutrients, and cellular movement.[3]

This 200 kDa membrane protein consists of six subunits, NqrA–F, all of which, except for NqrA, contain at least one transmembrane helix.[4,5] A noncovalently bound FAD and a [2Fe-2S] center are present in NqrF; two covalently bound FMNs are found in NqrB and NqrC, and the enzyme contains a molecule of riboflavin, probably in NqrB.[6,7] While riboflavin is often found as a precursor for the biosynthesis of FMN and

FAD,[8] in Na⁺-NQR riboflavin is an active cofactor involved in electron transfer.[7,9]

During the catalytic cycle, NADH donates electrons to the enzyme in a two-electron reaction, reducing the FAD cofactor to the flavohydroquinone form. Rapid time-resolved measurements have shown that one of these two electrons is subsequently transferred to the [2Fe-2S] center, producing an unstable neutral flavosemiquinone radical in FAD. From the [2Fe-2S] center, electrons flow through FMN_C, FMN_B, and riboflavin in a series of one-electron steps, before being donated to ubiquinone-8, a two-electron acceptor. In the oxidized "as-isolated" form of the enzyme, riboflavin is present as a stable one-electron neutral flavosemiquinone. Na⁺ uptake occurs during the step in which an electron is transferred from the

[2Fe-2S] center to FMN_C, while Na^+ efflux occurs during the FMN_B to riboflavin electron transfer step.[7,10−12]

The quinone reductase activity of Na^+-NQR follows Michaelis−Menten kinetics, with a K_m of 1−3 mM,[12] and is nearly saturated at a Na^+ concentration of 150 mM. In addition to Na^+, Na^+-NQR can also translocate lithium ions. Li^+ appears to bind at the same site(s) as Na^+, but the rate of catalytic turnover is only 140 s^{-1} in the presence of Li^+, as compared with 460 s^{-1} with Na^+.[13] Potassium ions are not translocated by the enzyme but have a regulatory effect. In the presence of Na^+, the addition of K^+ increases the catalytic activity and decreases the K_m, indicating that K^+ binds at a different site than Na^+.[13] On the other hand, Rb^+ binds at the same site as K^+ but inhibits catalytic turnover and decreases the affinity for Na^+.

Redox titrations of the wild-type enzyme have shown that, while the redox potentials of most of the cofactors are unaffected by the ionic composition of the medium, the potential of the FMN_C cofactor increases from −450 mV (vs Ag/AgCl) in the presence of K^+ and Rb^+ to −360 mV in the presence of Li^+ and Na^+.[14] It is interesting that this 90 mV shift occurs only in the presence of Na^+ and Li^+, the ions that Na^+-NQR is capable of translocating, suggesting that this coupling between the redox reactions and ion concentration is involved in catalysis.

A number of conserved acidic residues have been identified in transmembrane helices of NqrB, NqrD, and NqrE.[15] Three of these residues, NqrB-D397, NqrE-E95, and NqrD-D133, have been shown to participate in Na^+ binding, while four others are involved in Na^+ translocation and efflux.[15] Previous data for the ion dependence of the electrochemically induced Fourier transform infrared (FTIR) difference spectra of Na^+-NQR have revealed redox-induced changes that clearly involve acidic residues.[16] In this work, we have studied the interaction of different ions with wild-type Na^+-NQR and the NqrB-D397E mutant, using the same electrochemically induced FTIR difference spectroscopic approach. In other enzymes, this technique has been able to identify individual amino acids that participate in the reorganization that takes place upon the redox reaction and determine their protonation states.[17−19]

Ion translocation by Na^+-NQR has been proposed to involve conformational changes in the protein.[4] To study the influence of cations on enzyme conformation, we have monitored H−D exchange kinetics at the level of the amide protons. The approach is based on the observation that amide hydrogens in an open structure can exchange rapidly with solvent, whereas hydrogens involved in H-bonded structures, or when sterically inaccessible to the solvent, undergo exchange at slower rates.[20,21] Thus, the time course of H−D exchange gives information about the dynamics and flexibility of the enzyme under different conditions, as well as the influence of these ions on such conformational changes.[22−24] Altogether, the results of this work demonstrate the important role of conformational changes in the mechanism of Na^+-NQR, as well as the role of monodentate and bidentate carboxylates in sodium binding.

■ MATERIALS AND METHODS

Sample Preparation. Wild-type Na^+-NQR and the NqrB-D397E mutant were purified as reported previously.[15,25] Samples were prepared in 50 mM phosphate buffer (pH 8.0) and 0.05% dodecyl maltoside detergent, containing either 150 mM LiCl, NaCl, KCl, or RbCl, using Amicon centrifugal filters with a cutoff of 100 kDa. For experiments performed in the presence of Na^+ and Li^+, sodium phosphate and lithium

phosphate were used, respectively, whereas for experiments with K^+ and Rb^+, potassium phosphate buffer was used. The final concentration of the enzyme was approximately 0.75 mM, based on an absorption coefficient (ε_{ox-red}) of 36 mM^{-1} cm^{-1} at 460 nm.[26] For experiments performed in D_2O buffer, 15 μL of the protein was mixed with 400 μL of D_2O buffer and equilibrated for 5 h at 5 °C and then concentrated to the final volume.

Redox-Induced Mid-IR Difference Spectroscopic Studies. The electrochemically induced FTIR difference spectra were obtained as described previously.[16] The spectroelectrochemical cell has a three-electrode configuration. To avoid adsorption of protein to the working electrode, the gold grid was modified with a 2 mM aqueous solution of cysteamine and mercaptopropionic acid in a 1:1 ratio for at least 1 h. The redox reaction was accelerated by the presence of mediators at a final concentration of 15 μM as described previously.[27] The electrochemically induced FTIR difference spectra were recorded on a Vertex 70 FTIR spectrometer (Bruker) for the spectral range from 4000 to 1000 cm^{-1}. At the selected potential, the sample was equilibrated and then 2 × 256 scans at 4 cm^{-1} resolution were averaged. The reduction and oxidation of the enzyme, obtained for the potential step from −625 to 200 mV (vs Ag/AgCl; add 204 mV for SHE′), were then monitored after an equilibration time of 4 min for the full step. The full redox reaction was typically cycled 50−60 times, and the difference spectra were averaged. The temperature was fixed at 5 °C. The data were analyzed with respect to studies performed on model cofactors and individual amino acids.[19,27,28]

Hydrogen−Deuterium Exchange Kinetics. H−D exchange kinetics were monitored in the mid-IR region (1800−1400 cm^{-1}) in a Bruker Bio ATR Cell-2 instrument. The cell consists of two compartments separated by a dialysis membrane with a molecular mass cutoff of 3 kDa. The sample is placed on a Si-coated ZnSe ATR crystal in the lower compartment and equilibrated with a constant flow of H_2O buffer in the upper compartment, until consecutive spectra are constant. D_2O buffer (15 mL) was then pumped through the upper compartment at a flow rate of 0.2 mL/min, before a closed circuit with the D_2O buffer was set up. The temperature was maintained at 5 °C. Infrared spectra were recorded on a Bruker IFS28 spectrometer equipped with a DTGS detector. Data collection was started as soon as the D_2O buffer began to flow into the upper compartment. At the start of the exchange process, blocks of 16 consecutive spectra were recorded with 32, 64, 128, and 256 scans.[24] Finally, 72 spectra with 256 scans were recorded every 20 min. The experiment took ∼24 h. H−D exchange kinetics are monitored on the basis of the amide signals in the mid-infrared. The amide I signal involves contributions from the $\nu(C=O)$ vibrational mode of the polypeptide backbone, and the amide II signal involves the coupled $\nu(CN)/\delta(NH)$ vibrational mode. Upon H−D exchange, the amide II mode becomes uncoupled, and the $\delta(ND)$ vibrational mode undergoes a downshift. To accurately characterize the H−D exchange kinetics of the amide II mode, the following steps need to be taken. First, the contribution of the H_2O buffer must be subtracted from each recorded spectrum of the sample. Coefficients for subtraction were calculated according to eq 1.

$$a[H_2O] + b[D_2O] + c[HOD] = 1 \qquad (1)$$

With

$$a = \frac{\int_{2800}^{3800} S - \int_{2800}^{3800} D}{\int_{2800}^{3800} H - \int_{2800}^{3800} D}, \quad b = \frac{\int_{2200}^{2800} S - \int_{2200}^{2800} H}{\int_{2200}^{2800} D - \int_{2200}^{2800} H}, \quad c = 1 - a - b$$

where H is the spectrum of the sample in 100% H_2O, D is the last spectrum recorded for the experiment after buffer exchange, and S is the spectrum recorded at a given time that needs to be corrected. a, b, and c are the fractions of H_2O, D_2O, and HOD, respectively, present in the sample at any given time. a and b are calculated by integrating the recorded spectra in the given regions as described above. The H_2O buffer is then subtracted from each spectrum with the calculated coefficient. The next step is to normalize all the spectra according to the amide I signature, which is taken as an internal standard. The amount of protein in direct contact with the ATR crystal changes with time; the normalization step is based on the assumption that the amide I signature does not change in intensity through a 10 cm^{-1} downshift. The choice of amide I as an internal standard is also promoted by the fact that the amide I and amide II bands are separated by less than 50 cm^{-1}, thus reducing any baseline drift as a source of error. Finally, the amount of amide protons is calculated by dividing the integrated intensity of amide II by the integrated intensity of amide I at a given time. H−D exchange kinetics are analyzed by fitting this time course with eq 2

$$\frac{\left(\frac{\int_{1525}^{1575} \text{amide II}}{\int_{1600}^{1710} \text{amide I}}\right)_t}{\left(\frac{\int_{1525}^{1575} \text{amide II}}{\int_{1600}^{1710} \text{amide I}}\right)_0} = C_f \times \exp(-t/\tau_f) + C_s \times \exp(-t/\tau_s) + C_c \quad (2)$$

where C_f, C_s, and C_c are the fractions of amide protons attributed to the fast exchanging group, the slow exchanging group, and the protons that are not exchanged, respectively. τ_f and τ_s are the time constants for the fast and slow exchange kinetics, respectively. The amide II signal includes a contribution from tyrosine side chains. This is the main source of error upon comparison of the H−D exchange kinetics from different proteins with large differences in primary structure, as the limits for integrating the amide II component can differ; however, here we are comparing the same protein under different conditions, thus avoiding this problem.

■ RESULTS AND DISCUSSION

Electrochemically Induced FTIR Difference Spectra of Wild-Type Na⁺-NQR. The oxidized-minus-reduced FTIR difference spectra of wild-type Na⁺-NQR, in the presence of Na⁺, Li⁺, K⁺, and Rb⁺, are presented in Figure 1. The positive signals correlate with the oxidized form of the enzyme and the negative signals with the reduced form. The electrochemically induced FTIR difference spectra are expected to include overlapped contributions from the flavin cofactors, bound quinone and individual amino acids, as well as coupled protonation state changes and backbone reorganizations that take place during the redox reaction. It should be noted that the riboflavin cofactor only undergoes a one-electron redox transition; in the oxidized form of the enzyme riboflavin is
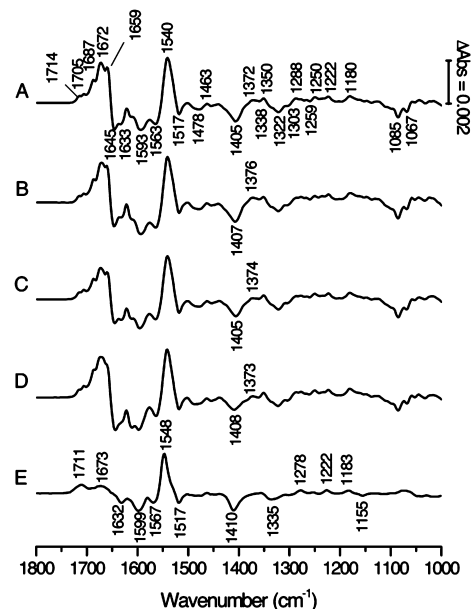
Figure 1. Oxidized-minus-reduced FTIR difference spectra of wild-type Na⁺-NQR in the presence of Na⁺ (A), Li⁺ (B), K⁺ (C), and Rb⁺ (D) in H_2O buffer, for the potential step from −620 to 100 mV (vs Ag/AgCl). The oxidized-minus-reduced difference spectrum of FAD (E) is also presented.

found as a stable one-electron reduced flavosemiquinone, while in the reduced form riboflavin is a two-electron reduced flavohydroquinone.[9,10] It is worth mentioning that the [2Fe-2S] clusters can also contribute, but at significantly lower frequencies.[29] The difference spectrum is characteristic of the protein and its redox reaction under specific conditions, which provides detailed information that can be used to study redox-linked conformational changes and the effects of mutations.

Three main regions can be distinguished in the spectra of Na⁺-NQR. (i) The $\nu(C=O)$ modes from the backbone are found in the amide I range between 1750 and 1600 cm^{-1}. These contributions are overlapped by other C=O vibrations, including those from flavins, quinones, and protonated Asp/Glu side chains. (ii) Between 1600 and 1500 cm^{-1}, the coupled $\nu(CN/NH)$ vibrations of the amide II modes are observed, together with contributions from the different amino acid side chains and the CN vibration of the flavins. (iii) At lower frequencies, in the so-called fingerprint region, the ring vibrations of the flavins are found together with the C−H and C−O vibrational modes of quinones and amino acid side chains. We note that several contributions overlap. For a detailed assignment of the signals, we compared the Na⁺-NQR spectra with those of individual cofactors, such as flavins and quinones, individual amino acids, or other proteins.

Figure 1A shows the difference spectra obtained in the presence of Na⁺, the naturally transported ion in Na⁺-NQR. The oxidized-minus-reduced spectrum of FAD is shown in Figure 1E to help in identifying the contributions of the flavin cofactors. The flavins dominate the electrochemically induced FTIR difference spectra of Na⁺-NQR.[27] At 1714 and 1705 cm^{-1}, the $\nu(C=O)$ modes of the flavins are seen together with signals from the protonated carboxylic groups of Asp/Glu acid side chains.[27,30] Positive signals at 1687, 1672, and 1659 cm^{-1} and negative signals at 1645, 1633, and 1612 cm^{-1} can be attributed to the amide I contribution, arising from the $\nu(C=O)$ mode of the polypeptide backbone, reflecting conforma-

tional changes that are coupled to the oxidoreduction of the cofactors. The $\nu(C=O)$ vibrational modes of neutral flavosemiquinone are involved in the large positive feature at 1659 cm^{-1}. In addition, the signal at 1687 cm^{-1} is at a position typical for the $\nu(C=O)$ mode of Gln and Asn and the $\nu_{as}(CN_3H_5^+)$ vibration of Arg side chains. The signal at 1631 cm^{-1} may involve the $\nu_s(CN_3H_5^+)$ vibrational mode of Arg side chains.[28,31,32] In the amide II region, between 1590 and 1520 cm^{-1}, the coupled $\nu(C=N)/\delta(N-H)$ vibrational modes of the polypeptide backbone are seen at 1593 and 1563 cm^{-1}, together with the $\nu(C=N)$ vibrational modes of the flavin cofactors. At 1540 cm^{-1}, a prominent signal can be found at a position typical for the $\nu(C=C)$ vibrational modes of neutral flavosemiquinone. The $\nu_{as}(COO^-)$ vibrational modes of deprotonated Glu/Asp side chains may also contribute to the signals at 1593, 1563, and 1540 cm^{-1}.[28,31,32] The $\nu_s(COO^-)$ modes of the deprotonated acidic residues contribute at 1405 and 1372 cm^{-1}. These signals also include modes arising from reorganization of the isoalloxazine ring system of the flavins, as seen in Figure 1E.[27,33] The signal at 1517 cm^{-1}, observed for the reduced form, is also seen in the difference spectra of FAD and has been attributed to the $\delta(C-H)^{in\ plane}/\delta(N-H)^{in\ plane}$ mode of flavins.[27,33] Between 1400 and 1200 cm^{-1}, small signals arising from isoalloxazine ring rearrangement can be observed. Signals typical of the $C-OCH_3$ vibrational modes of the methoxy groups of the bound quinone are expected between 1250 and 1270 cm^{-1}.[34]

Oxidized-minus-reduced FTIR difference spectra B–D of Figure 1 were obtained in the presence of Li$^+$, K$^+$, and Rb$^+$, respectively. The general shape of the redox-induced difference spectra is not altered by the ion present. Nevertheless, small but significant changes are observed. To highlight these shifts, double-difference spectra, calculated by subtracting the difference spectra in Figure 1, are presented in Figure 2.
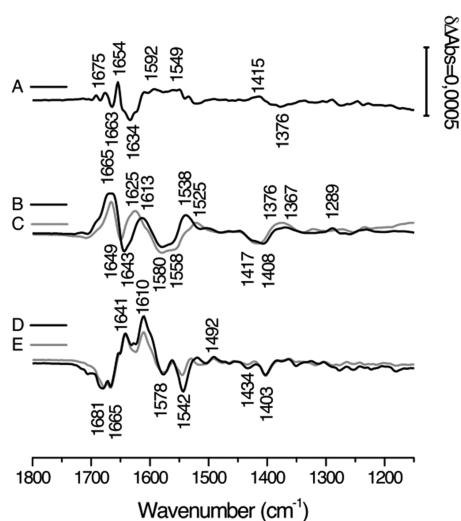
The Na$^+$-minus-Li$^+$ double-difference spectrum, obtained by interactively subtracting the oxidized-minus-reduced difference spectrum in the presence of Li$^+$ from that in the presence of Na$^+$, is presented in Figure 2A. Signals at 1675, 1663, and 1634

cm^{-1} reveal alterations in redox-linked conformational changes, mainly involving β-sheets and turns, upon the change from Li$^+$ to Na$^+$.[35,36,39] At 1654 cm^{-1}, a sharp positive signal is observed in the presence of Na$^+$ that may be attributed to α-helical structures that shift upon ion binding. Our previous experiments demonstrated that sodium and lithium occupy the same binding site and have a similar affinity. However, the activity with sodium is 3 times higher than that with lithium, which indicates that the enzyme presents other selectivity filters downstream of the sodium binding site(s). The structural changes represented in Figure 2A account for such changes, which possibly involve one or more transmembrane helices that could form the cation pathway.

The $\nu_{as}(COO^-)$ vibrational mode of deprotonated acidic residues is expected in the region between 1600 and 1540 cm^{-1} and may be involved in the signal at 1549 cm^{-1}, along with amide II vibrational modes. At 1415 and 1376 cm^{-1}, the $\nu_s(COO^-)$ vibrational modes of deprotonated Asp/Glu acidic side chains are expected.[28,31,32] COO$^-$ groups, when coordinated with metal ions, show frequencies similar to those of the deprotonated acidic residues. The observed difference in the carboxylic acid signals in the presence of Na$^+$ and Li$^+$ can be explained by differences in ligation between the two ions, because sodium is typically bound by six ligands, arranged in an octahedral geometry, while lithium is bound by five.

The Na$^+$-minus-K$^+$ and Li$^+$-minus-K$^+$ double-difference spectra (Figure 2B,C) show similar shapes. This data set is important in our characterization because it shows the effect of sodium (and lithium) binding on the conformation of the enzyme, compared with the enzyme in a high-ionic strength medium, but with unoccupied catalytic binding sites. A large signal is observed at 1665 cm^{-1} representative of changes in secondary structural elements. In the Na$^+$-minus-K$^+$ double-difference spectrum, a negative signal at 1643 cm^{-1} and a positive signal at 1613 cm^{-1} are observed in the amide I region. Similar contributions are seen in the Li$^+$-minus-K$^+$ double-difference spectrum at 1649 and 1625 cm^{-1}. In the amide II spectral range, contributions from the backbone, and from deprotonated acidic residues, overlap at 1580 and 1558 cm^{-1}. In addition to the general changes in structure upon sodium and lithium binding, we were also able to study the effect of these cations on the binding sites, by following the carboxylate signals. Negative signals at 1417 and 1408 cm^{-1} and positive signals at 1376 and 1367 cm^{-1} in both the Na$^+$-minus-K$^+$ and Li$^+$-minus-K$^+$ spectra can be attributed to the $\nu_s(COO^-Li^+)$ and $\nu_s(COO^-Na^+)$ modes of acidic residue side chains.[37,38,40] The positions are essentially identical, indicating that the environment of the COO$^-$ group is very similar for Li$^+$ and Na$^+$. The absence of signals in the region above 1710 cm^{-1} suggests that no protonated acidic residues are interacting with the ions.[28,30−32]

The effect of Rb$^+$ was also studied, because this ion binds at the same site as K$^+$ but inhibits the activity of the enzyme. The Na$^+$-minus-Rb$^+$ and K$^+$-minus-Rb$^+$ FTIR double-difference spectra (Figure 2D,E) show a clear influence of Rb$^+$ on signals in the amide I region at 1681, 1665, 1641, and 1610 cm^{-1}. In addition to changes of the conformational reorganization of the enzyme upon oxidoreduction, the $\nu_{as}(COO^-Rb^+)$ vibrational mode can be identified at 1578 cm^{-1}. The negative signal at 1403 cm^{-1} can be attributed to $\nu_s(COO^-Rb^+)$ and suggests that Rb$^+$ is bound to the protein in the reduced form.

Figure 2. Double-difference spectra comparing the oxidized-minus-reduced FTIR difference spectra of wild-type Na$^+$-NQR in H$_2$O buffer, in the presence of different monovalent cations: Na$^+$ minus Li$^+$ (A), Na$^+$ minus K$^+$ (B), Li$^+$ minus K$^+$ (C), Na$^+$ minus Rb$^+$ (D), and K$^+$ minus Rb$^+$ (E).

Table 1. Tentative Assignments of the Signals Observed in the Oxidized-minus-Reduced Difference Spectra of the Na⁺-NQR Wild-Type Protein in H₂O and D₂O Buffer[a]

| position (cm⁻¹)		tentative attribution
samples prepared in H₂O	samples prepared in D₂O	
1714 (+)		$\nu(C{=}O)$ of Asp/Glu, $\nu(C_4{=}O)$ of flavins
1705 (+)	1704 (+)	$\nu(C{=}O)$ of Asp/Glu, $\nu(C_4{=}O)$ of flavins
1687 (+)	1687 (+)	amide I; β-turn, $\nu(C_2{=}O)$ of flavins, Arg $\nu_{as}(CN_3H_5)$
1672 (+)	1664 (+)	amide I; β-turn, $\nu(C_2{=}O)$ of flavins, $\nu(C{=}O)$ of quinone, $\nu(C{=}O)$ of Gln, Asn
1659 (+)		amide I; α-helix, $\nu(C{=}O)$ of flavins
1645 (−)		amide I; random structures, $\nu(C_4{=}O)$ of flavins
1633 (−)	1637 (+)	amide I; β-sheet, $\nu(C_4{=}O)$ of flavins, Arg $\nu_s(CN_3H_5)$
1593 (−)	1589 (−)	$\nu_{as}(COO^-)$ of Asp/Glu, $\nu(C_{10a}{=}N_1)$, $\nu(C_{4a}{=}N_5)$ of flavins
1563 (−)	1561 (−)	amide II; $\nu_{as}(COO^-)$ of Asp/Glu, $\nu(C_{10a}{=}N_1)$, $\nu(C_{4a}{=}N_5)$ of flavins
1540 (+)	1539 (+)	amide II; $\nu_{as}(COO^-)$ of Asp/Glu, $\nu(C{=}C)$ of neutral flavins
1517 (−)	1512 (−)	$\delta(C{-}H)^{in\ plane}/\delta(N{-}H)^{in\ plane}$ of flavins
1478 (−)	1463 (+)	$\delta_{as}(C{-}H_3)$
1463 (+)	1445 (+)	$\delta_{as}(C{-}H_3)$
1404 (−)	1402 (−)	$\nu_s(COO^-)$ of Asp/Glu, isoalloxazine ring reorganization
1372 (+)	1372 (+)	$\nu_s(COO^-)$ of Asp/Glu
1350 (+)	1351 (+)	
1338 (−)	1335 (−)	$\delta(C{-}H)$, ring flavins
1322 (−)		$\delta(C{-}H)$, ring flavins
1303 (−)		$\delta(C{-}H)$, ring flavins
1300−1100 (+)	1300−1000 (+)	several overlapping small contributions, including ring flavins, C−OCH₃ quinone, Tyr and other amino acids
1085 (−)	1100 (−)	$\nu(P{=}O)$ of phosphate buffer
1067 (−)	1071 (−)	$\nu(P{=}O)$ of phosphate buffer

[a]Plus signs indicate positive signals, and minus signs indicate negative signals. The references supporting these tentative assignments are given in the text.

To confirm the tentative assignments discussed above, and summarized in Table 1, we repeated the experiments in D₂O buffer. These control experiments can be found in the Supporting Information.

Electrochemically Induced FTIR Difference Spectra of the NqrB-D397E Mutant. Our previous studies of acidic residue mutants showed that the NqrB-D397 residue plays a part in at least one Na⁺ binding site in Na⁺-NQR. To gain further insight into the functional ion binding site(s) of the enzyme, we studied a mutant in which this residue was substituted with glutamic acid. The original mutation at this position, NqrB-D397A, led to a severely decreased rate of turnover, resulting from inhibition of the [2Fe-2S] → FMN$_C$ internal electron transfer step, accompanied by large changes in Na⁺ dependence.[15] These results were interpreted as showing that NqrB-D397 is part of the initial Na⁺ uptake site. Initial FTIR measurements on the NqrB-D397A mutant showed noticeable perturbation of the contribution from the flavins. For this investigation, we have chosen to study a mutant in which NqrB-D397 has been replaced with glutamic acid. This substitution alters the size, but not the functional group, producing an enzyme that presents ∼25% of the activity (M. E. Shea et al., manuscript in preparation).
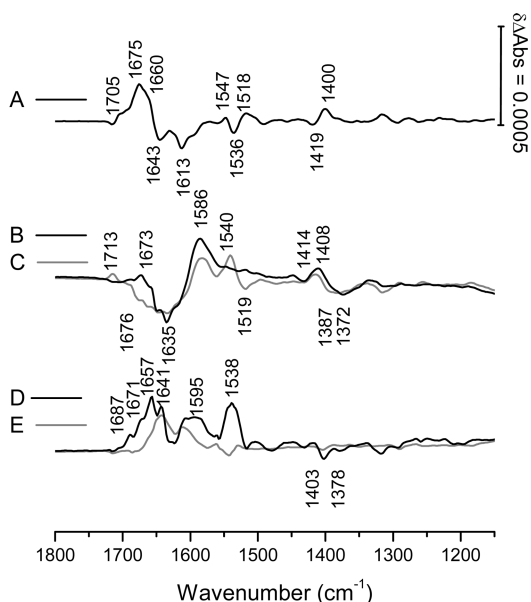
Figure 3 shows the oxidized-minus-reduced FTIR difference spectra of the NqrB-D397E mutant enzyme in the presence of different monovalent cations. The difference spectra are similar to those obtained with the wild-type protein, confirming the structural integrity of the mutant enzyme. To depict the effects of the different ions on the redox-induced difference spectra, interactive subtraction of the mutant data obtained in the presence of the different ions was performed to yield double-difference spectra (Figure 4). Together with the double-difference spectra (Figure 5), obtained by subtracting the
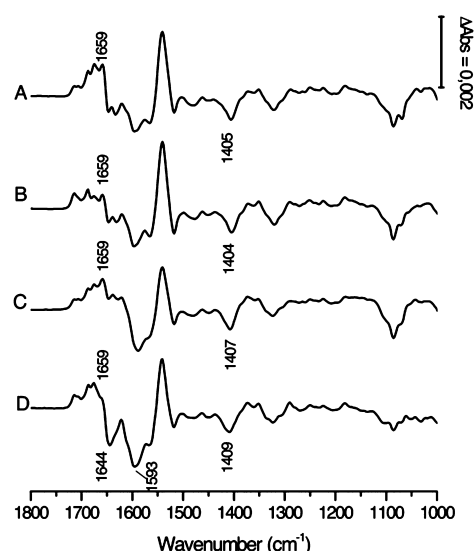

Figure 3. Oxidized-minus-reduced FTIR difference spectra of the NqrB-D397E mutant enzyme in the presence of Na⁺ (A), Li⁺ (B), K⁺ (C), and Rb⁺ (D) for the potential step from −620 to 200 mV (vs Ag/AgCl) in H₂O buffer.

spectra of the mutant (Figure 3) from that of the wild-type enzyme (Figure 1), the shifts and different interaction features in the mutant can be highlighted. Importantly, an additional signal appears at 1714 cm⁻¹, at a position typical for the $\nu(C{=}O)$ modes of protonated Asp and Glu residues. We suggest that this reflects the protonation of one of the acidic residues participating in ion binding as a result of the mutation.

For the data in the presence of Na⁺, changes in the conformation of the protein are seen in the amide I region at

Figure 4. Double-difference spectra comparing oxidized-minus-reduced FTIR difference spectra of the NqrB-D397E mutant enzyme in the presence of different salts: Na$^+$ minus Li$^+$ (A), Na$^+$ minus K$^+$ (B), Li$^+$ minus K$^+$ (C), Na$^+$ minus Rb$^+$ (D), and K$^+$ minus Rb$^+$ (E).
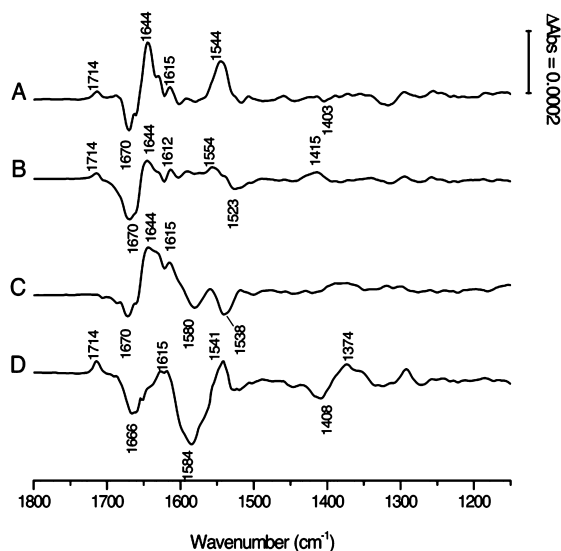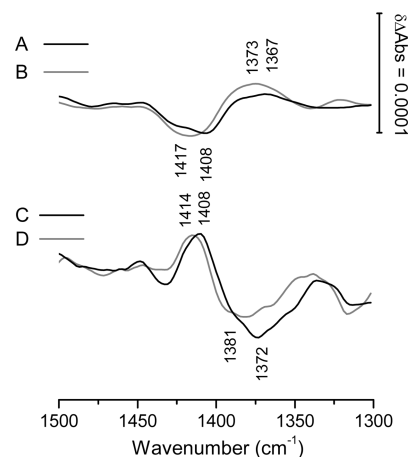

Figure 5. Double-difference spectra of the D397E mutant minus the wild type with Na$^+$ (A), Li$^+$ (B), K$^+$ (C), and Rb$^+$ (D).

1670 and 1644 cm^{-1}. These signals correspond to β-turn and β-sheet structures or involve the contributions of arginine.[35] Interestingly, these difference signals are also observed in the presence of Li$^+$ and K$^+$ and are therefore independent of the type of ions present in the sample, but specific to the mutation. In the complex spectral range where the $\nu_{as}(COO^-)$ vibrational modes from Asp/Glu side chains, the $\nu(C=O)$ vibration of the flavins, and the amide II vibrations overlap, a positive signal is seen at 1544 cm^{-1} in the presence of Na$^+$. This shift is seen in the data for all ions, but with varying intensity. Because the flavins are relatively unperturbed in the mutant, and parallel measurements of the wild type in D$_2$O show H−D exchange excluding any significant amide II contributions (see Figures 1 and 2 of the Supporting Information), the most likely origin of this shift is the perturbation of a COO$^-$ group. In the presence

of Li$^+$, the general shape of the double-difference spectrum is similar to the shape of that obtained in the presence of Na$^+$. In the amide II region, a positive component is observed at 1554 cm^{-1}, 10 cm^{-1} higher than in the presence of Na$^+$. For samples studied in the presence of K$^+$, two negative signals are observed in the amide II region at 1580 and 1538 cm^{-1}. These signals are representative of the perturbation of the coordination system of Na$^+$ in the NqrB-D397E mutant enzyme.

Upon comparison of the data to results obtained for the wild-type enzyme, it becomes evident that a major change has occurred. The order of the frequencies of the $\nu_s(COO^-)$ vibrational modes is inverted for the different ions studied. These changes are highlighted in Figure 6. Because at least

Figure 6. Double-difference spectra in the spectral range between 1500 and 1300 cm^{-1} of the wild-type enzyme [Na$^+$ minus K$^+$ (A) and Li$^+$ minus K$^+$ (B)] and the NqrB-D397E mutant protein [Na$^+$ minus K$^+$ (C) and Li$^+$ minus K$^+$ (D)].

three carboxylic groups are typically needed for alkali metal cation binding, the NqrB-D397E mutation may affect the strength of binding between the ions and the amino acid ligands. The upshift observed suggests that binding of Na$^+$ and Li$^+$ is weakened in the NqrB-D397E mutant enzyme.

The inhibitor Rb$^+$ also interacts differently in the mutant and the wild type. An additional large negative signal at 1666 cm^{-1} is observed in the amide I range. Furthermore, a large negative signal is also observed in the amide II region at 1584 cm^{-1} and a positive band is observed at 1541 cm^{-1}. At a lower frequency, a strong perturbation of the $\nu_s(COO^-)$ modes of Asp/Glu side chains is seen at 1408 and 1374 cm^{-1}. For this ion, a major change in the features due to interaction with the acidic residues is apparent upon comparison of the mutant and the wild type.

Hydrogen−Deuterium Exchange Kinetics. In previous studies, we have proposed that conformational changes are involved in coupling electron transfer to ion translocation in Na$^+$-NQR. To further investigate this mechanism, we performed H−D exchange kinetic measurements in the presence of Na$^+$, Li$^+$, K$^+$, and Rb$^+$ with the wild-type Na$^+$-NQR and NqrB-D397E mutant enzymes. Generally, the H−D exchange kinetics of amide protons are followed by measuring the decrease in the magnitude of the amide II signal in the infrared absorption spectrum, during the exchange process. These measurements reveal the degree to which protons in an enzyme are accessible to solvent exchange, which can provide important information about the conformations of proteins that

Table 2. Analysis of the H−D Exchange Kinetics of Wild-Type Na⁺-NQR and the NqrB-D397E Mutant Protein in the Presence of Li⁺, Na⁺, K⁺, and Rb⁺

sample	exchange kinetics	Na⁺ %	Na⁺ time	Li⁺ %	Li⁺ time	K⁺ %	K⁺ time	Rb⁺ %	Rb⁺ time
wild type	fast	40	10	41	10	37	10	37	10
	slow	6	150	5	400	5	250	4	415
	hydrophobic core	54	–	54	–	58	–	59	–
NqrB-D397E	fast	39	10	37	10	37	10	38	10
	slow	8	300	5	200	2	200	–	–
	hydrophobic core	53	–	58	–	61	–	62	–

would not be otherwise observed.[21] Three different groups of amide protons can be typically found: a fast exchanging group, which corresponds to the amide protons on the surface of the protein that are readily available for H−D exchange,[20,21] a slower exchanging group, which includes amide protons, either just beneath the surface or in hydrophilic cavities, and, finally, a population of amide protons that effectively do not exchange with solvent, either because they are in the hydrophobic core, for example, in transmembrane helices, or because they are involved in strong hydrogen bonding, even though they may be located at the surface of the protein.[41]

H−/D exchange was measured in wild-type Na⁺-NQR, in the presence the four different ions, Li⁺, Na⁺, K⁺, and Rb⁺, to determine their effect on the accessibility of the amide protons, which could indicate conformational flexibility of the protein. A plot of the fraction of amide protons versus time upon H−D buffer exchange for the wild-type enzyme (top) and the NqrB-D397E mutant (bottom) was analyzed using eq 2, and the results are expressed in terms of percentages of the three populations described above (Table 2). The original data are given in the Supporting Information.

The effects of the different ions can be divided into two distinct categories. In the presence of Li⁺ and Na⁺, 54% of the amide protons are not accessible to the solvent. The fast exchange phase in both cases includes 40% of the amide protons. In the presence of the nontransported ions, K⁺ and Rb⁺, the time constant for the fast exchange kinetics is 10 min, which is similar to that in the presence of Na⁺ and K⁺. The relative contribution decreased from 40 to 37%. Interestingly, the change involves the contribution of protons in the hydrophobic core, which increases from 54 to 58%. Although the changes might be considered small, it should be taken into account that a 4−5% change may involve a large conformational change that can expose a domain, or open a channel, that accounts for $^1/_{20}$ of the protein total surface. Thus, these effects confirm that the enzyme can adopt several conformational states that have different accessibilities to the aqueous environment, as we have proposed.[10]

In the NqrB-D397E mutant enzyme, the solvent accessibility is closely related to the type of ions present in the sample. Amide protons are most accessible in the presence of Na⁺ and Li⁺. Rb⁺ acts as an inhibitor of the enzyme, and H−D exchange shows that the NqrB-D397E mutant enzyme is less accessible in the presence of Rb⁺.

CONCLUSION

Na⁺-NQR is a unique redox-driven respiratory enzyme that conserves energy by selectively pumping Na⁺ across the bacterial membrane but is also capable of translocating Li⁺. The enzyme contains up to three different sodium binding sites, with K_d values of 2−3 mM, which show positive cooperativity.[13] Other monovalent cations are not transported by the enzyme, although K⁺ is a regulator that stimulates enzyme turnover, through the binding to a site different from that of Na⁺ and Li⁺. Rb⁺ binds at the same site as K⁺ but has an inhibitory effect.[13] Recently, it was shown that the midpoint potential of the FMN_C cofactor in Na⁺-NQR from *V. cholerae* increases by 90 mV in the presence of Na⁺ and Li⁺, in comparison to that in the presence of K⁺, which demonstrates that the mechanism of sodium transport is partially thermodynamically controlled.[14] In this report, we have characterized the structural factors that are involved in sodium binding and transport, through FTIR redox-induced spectroscopy. We recently proposed that the Na⁺ pumping mechanism of Na⁺-NQR involves a series of conformational changes by which the uptake of Na⁺, its translocation across the membrane, and its release to the periplasmic space are coupled to the redox reactions of the enzyme.

The results clearly demonstrate that the process of electron transfer, probably between the redox centers that control sodium binding and release, produces conformational changes that are involved in sodium transport. This supports our earlier proposal that conformational changes are an important part of an indirect coupling mechanism that allows the redox reaction of Na⁺-NQR to drive the pumping of Na⁺.

This study has made it possible to assign the FTIR spectra of Na⁺-NQR and importantly has revealed the role of carboxylates in binding of sodium and lithium. The $\nu_s(COO^-M^+)$ signals observed in the oxidized form of wild-type Na⁺-NQR suggest that the interaction is monodentate, while in the reduced form, the carboxylates are bidentate ligands. This bidentate interaction may contribute to the regulation of sodium uptake, as previously suggested. In the NqrB-D397E mutant enzyme, the order of the frequencies of the $\nu_s(COO^-)$ vibrational modes in the presence of the different ions is inverted. Because six ligands are typically required for Na⁺ binding, replacing NqrB-D397 with the larger glutamate residue may affect the relative strengths of the bonds between the ions and the residues involved in binding. The shifts observed suggest that Na⁺ binding and Li⁺ binding are both weakened in the NqrB-D397E mutant enzyme.

■ ASSOCIATED CONTENT

ⓈSupporting Information

Oxidized-minus-reduced FTIR difference spectra of wild-type Na⁺-NQR in the presence of Na⁺, Li⁺, K⁺, and Rb⁺ in D₂O buffer and the respective double-difference spectra together with the evolution of the fraction of amide protons versus time in the presence of Na⁺, Li⁺, K⁺, and Rb⁺ for wild-type Na⁺-NQR and the NqrB-D397E mutant. This material is available free of charge via the Internet at http://pubs.acs.org.

■ AUTHOR INFORMATION

Corresponding Author

*Laboratoire de bioelectrochimie et spectroscopie, UMR 7140, Chimie de la Matière Complexe, Université de Strasbourg-CNRS, 1 Rue Blaise Pascal, 67070 Strasbourg, France. Telephone: 00 33 3 68 85 12 73. Fax: 00 33 3 68 85 1662. E-mail: hellwig@unistra.fr.

Notes

The authors declare no competing financial interest.

■ ABBREVIATIONS

Na$^+$-NQR, Na$^+$-pumping NADH:quinone oxidoreductase; ΔAbs, difference in absorbance.

■ REFERENCES

(1) Dimroth, P., and Thomer, A. (1989) A primary respiratory Na$^+$ pump of an anaerobic bacterium: The Na$^+$-dependent NADH:quinone oxidoreductase of *Klebsiella pneumoniae*. *Arch. Microbiol.* 151, 439–444.

(2) Hayashi, M., and Unemoto, T. (1984) Characterization of the Na$^+$-dependent respiratory chain NADH:quinone oxidoreductase of the marine bacterium, *Vibrio alginolyticus*, in relation to the primary Na$^+$ pump. *Biochim. Biophys. Acta* 767, 470–478.

(3) Häse, C. C., and Barquera, B. (2001) Role of sodium bioenergetics in *Vibrio cholerae*. *Biochim. Biophys. Acta* 1505, 169–178.

(4) Juárez, O., and Barquera, B. (2012) Insights into the mechanism of electron transfer and sodium translocation of the Na$^+$-pumping NADH:quinone oxidoreductase. *Biochim. Biophys. Acta* 1817, 1823–1832.

(5) Verkhovsky, M. I., and Bogachev, A. V. (2010) Sodium-translocating NADH:quinone oxidoreductase as a redox-driven ion pump. *Biochim. Biophys. Acta* 1797, 738–746.

(6) Backiel, J., Juarez, O., Zagorevski, D. V., Wang, Z., Nilges, M. J., and Barquera, B. (2008) Covalent binding of flavins to RnfG and RnfD in the Rnf complex from *Vibrio cholerae*. *Biochemistry* 47, 11273–11284.

(7) Barquera, B., Ramirez-Silva, L., Morgan, J. E., and Nilges, M. J. (2006) A new flavin radical signal in the Na$^+$-pumping NADH:quinone oxidoreductase from *Vibrio cholerae*: An EPR/electron nuclear double resonance investigation of the role of the covalently bound flavins in subunits B and C. *J. Biol. Chem.* 281, 36482–36491.

(8) MacHeroux, P., Kappes, B., and Ealick, S. E. (2011) Flavogenomics: A genomic and structural view of flavin-dependent proteins. *FEBS J.* 278, 2625–2634.

(9) Juárez, O., Nilges, M. J., Gillespie, P., Cotton, J., and Barquera, B. (2008) Riboflavin is an active redox cofactor in the Na$^+$-pumping NADH:quinone oxidoreductase (Na$^+$-NQR) from *Vibrio cholerae*. *J. Biol. Chem.* 283, 33162–33167.

(10) Juárez, O., Morgan, J. E., Nilges, M. J., and Barquera, B. (2010) Energy transducing redox steps of the Na$^+$-pumping NADH:quinone oxidoreductase from *Vibrio cholerae*. *Proc. Natl. Acad. Sci. U.S.A.* 107, 12505–12510.

(11) Bogachev, A. V., Bertsova, Y. V., Barquera, B., and Verkhovsky, M. I. (2001) Sodium-dependent steps in the redox reactions of the Na$^+$-motive NADH:quinone oxidoreductase from *Vibrio harveyi*. *Biochemistry* 40, 7318–7323.

(12) Juárez, O., Neehaul, Y., Turk, E., Chahboun, N., DeMicco, J. M., Hellwig, P., and Barquera, B. (2012) The role of glycine residues 140 and 141 of subunit B in the functional ubiquinone binding site of the Na$^+$-pumping NADH:quinone oxidoreductase from *Vibrio cholerae*. *J. Biol. Chem.* 287, 25678–25685.

(13) Juárez, O., Shea, M. E., Makhatadze, G. I., and Barquera, B. (2011) The role and specificity of the catalytic and regulatory cation-binding sites of the Na$^+$-pumping NADH:quinone oxidoreductase from *Vibrio cholerae*. *J. Biol. Chem.* 286, 26383–26390.

(14) Neehaul, Y., Juárez, O., Barquera, B., and Hellwig, P. (2012) Thermodynamic contribution to the regulation of electron transfer in the Na$^+$-pumping NADH:Quinone oxidoreductase from *Vibrio cholerae*. *Biochemistry* 51, 4072–4077.

(15) Juárez, O., Athearn, K., Gillespie, P., and Barquera, B. (2009) Acid residues in the transmembrane helices of the Na$^+$-pumping NADH:quinone oxidoreductase from *Vibrio cholerae* involved in sodium translocation. *Biochemistry* 48, 9516–9524.

(16) Friedrich, T., Stolpe, S., Schneider, D., Barquera, B., and Hellwig, P. (2005) Ion translocation by the *Escherichia coli* NADH:ubiquinone oxidoreductase (complex I). *Biochem. Soc. Trans.* 33, 836–839.

(17) Hellwig, P., Behr, J., Ostermeier, C., Richter, O. M., Pfitzner, U., Odenwald, A., Ludwig, B., Michel, H., and Mantele, W. (1998) Involvement of glutamic acid 278 in the redox reaction of the cytochrome c oxidase from *Paracoccus denitrificans* investigated by FTIR spectroscopy. *Biochemistry* 37, 7390–7399.

(18) Hellwig, P., Rost, B., Kaiser, U., Ostermeier, C., Michel, H., and Mantele, W. (1996) Carboxyl group protonation upon reduction of the *Paracoccus denitrificans* cytochrome c oxidase: Direct evidence by FTIR spectroscopy. *FEBS Lett.* 385, 53–57.

(19) Barth, A. (2007) Infrared spectroscopy of proteins. *Biochim. Biophys. Acta* 1767, 1073–1101.

(20) Benson, E. E., and Linderstrøm-Lang, K. (1959) Deuterium exchange between myoglobin and water. *Biochim. Biophys. Acta* 32, 579–581.

(21) Englander, S. W., Sosnick, T. R., Englander, J. J., and Mayne, L. (1996) Mechanisms and uses of hydrogen exchange. *Curr. Opin. Struct. Biol.* 6, 18–23.

(22) Goormaghtigh, E., Cabiaux, V., and Ruysschaert, J. M. (1994) Determination of soluble and membrane protein structure by Fourier transform infrared spectroscopy. II. Experimental aspects, side chain structure, and H/D exchange. *Subcell. Biochem.* 23, 363–403.

(23) Džafić, E., Klein, O., Screpanti, E., Hunte, C., and Mäntele, W. (2009) Flexibility and dynamics of NhaA Na$^+$/H$^+$-antiporter of *Escherichia coli* studied by Fourier transform infrared spectroscopy. *Spectrochim. Acta, Part A* 72, 102–109.

(24) Hielscher, R., Friedrich, T., and Hellwig, P. (2011) Far- and Mid-Infrared Spectroscopic Analysis of the Substrate-Induced Structural Dynamics of Respiratory Complex I. *ChemPhysChem* 12, 217–224.

(25) Barquera, B., Hellwig, P., Zhou, W., Morgan, J. E., Hase, C. C., Gosink, K. K., Nilges, M., Bruesehoff, P. J., Roth, A., Lancaster, C. R., and Gennis, R. B. (2002) Purification and characterization of the recombinant Na$^+$-translocating NADH:quinone oxidoreductase from *Vibrio cholerae*. *Biochemistry* 41, 3781–3789.

(26) Juárez, O., Morgan, J. E., and Barquera, B. (2009) The electron transfer pathway of the Na$^+$-pumping NADH:Quinone oxidoreductase from *Vibrio cholerae*. *J. Biol. Chem.* 284, 8963–8972.

(27) Hellwig, P., Scheide, D., Bungert, S., Mantele, W., and Friedrich, T. (2000) FT-IR spectroscopic characterization of NADH:ubiquinone oxidoreductase (complex I) from *Escherichia coli*: Oxidation of FeS cluster N2 is coupled with the protonation of an aspartate or glutamate side chain. *Biochemistry* 39, 10884–10891.

(28) Wolpert, M., and Hellwig, P. (2006) Infrared spectra and molar absorption coefficients of the 20 α amino acids in aqueous solutions in the spectral range from 1800 to 500 cm^{-1}. *Spectrochim. Acta, Part A* 64, 987–1001.

(29) El Khoury, Y., and Hellwig, P. (2011) A combined far-infrared spectroscopic and electrochemical approach for the study of iron-sulfur proteins. *ChemPhysChem* 12, 2669–2674.

(30) Siebert, F., Mäntele, W., and Kreutz, W. (1982) Evidence for the protonation of two internal carboxylic groups during the photocycle of bacteriorhodopsin. Investigation of kinetic infrared spectroscopy. *FEBS Lett. 141*, 82−87.

(31) Venyaminov, S. Y., and Kalnin, N. N. (1990) Quantitative IR spectrophotometry of peptide compounds in water (H_2O) solutions. I. Spectral parameters of amino acid residue absorption bands. *Biopolymers 30*, 1243−1257.

(32) Barth, A. (2000) The infrared absorption of amino acid side chains. *Prog. Biophys. Mol. Biol. 74*, 141−173.

(33) Wille, G., Ritter, M., Friedemann, R., Mäntele, W., and Hübner, G. (2003) Redox-Triggered FTIR Difference Spectra of FAD in Aqueous Solution and Bound to Flavoproteins. *Biochemistry 42*, 14814−14821.

(34) Hellwig, P., Mogi, T., Tomson, F. L., Gennis, R. B., Iwata, J., Miyoshi, H., and Mäntele, W. (1999) Vibrational modes of ubiquinone in cytochrome bo_3 from *Escherichia coli* identified by Fourier transform infrared difference spectroscopy and specific ^{13}C labeling. *Biochemistry 38*, 14683−14689.

(35) Goormaghtigh, E., Cabiaux, V., and Ruysschaert, J. M. (1994) Determination of soluble and membrane protein structure by Fourier transform infrared spectroscopy. III. Secondary structures. *Subcell. Biochem. 23*, 405−450.

(36) Venyaminov, S. Y., and Kalnin, N. N. (1990) Quantitative IR spectrophotometry of peptide compounds in water (H_2O) solutions. II. Amide absorption bands of polypeptides and fibrous proteins in α-, β-, and random coil conformations. *Biopolymers 30*, 1259−1271.

(37) Nara, M., Torii, H., and Tasumi, M. (1996) Correlation between the vibrational frequencies of the carboxylate group and the types of its coordination to a metal ion: An ab initio molecular orbital study. *J. Phys. Chem. 100*, 19812−19817.

(38) Nara, M., Tasumi, M., Tanokura, M., Hiraoki, T., Yazawa, M., and Tsutsumi, A. (1994) Infrared studies of interaction between metal ions and Ca^{2+}-binding proteins. Marker bands for identifying the types of coordination of the side-chain COO^- groups to metal ions in pike parvalbumin (pI = 4.10). *FEBS Lett. 349*, 84−88.

(39) Goormaghtigh, E., Cabiaux, V., and Ruysschaert, J. M. (1994) Determination of soluble and membrane protein structure by Fourier transform infrared spectroscopy. I. Assignments and model compounds. *Subcell. Biochem. 23*, 329−362.

(40) Deacon, G. B., Huber, F., and Phillips, R. J. (1985) Diagnosis of the nature of carboxylate coordination from the direction of shifts of carbonoxygen stretching frequencies. *Inorg. Chim. Acta 104*, 41−45.

(41) Earnest, T. N., Herzfeld, J., and Rothschild, K. J. (1990) Polarized Fourier transform infrared spectroscopy of bacteriorhodopsin. Transmembrane α helices are resistant to hydrogen/deuterium exchange. *Biophys. J. 58*, 1539−1546.